

Diagnostic Significance of Conventional and Advanced Neuroimaging in Sturge-Weber Syndrome and Related Brain Abnormalities: An Overview

Santosh Kumar Bhagat M.D.¹, Jing Tao Wu M.D., Ph.D¹, Ye Jing M.D.^{1†},
Ying Wen Zhou M.D.¹, SarojKafle MD.², ZafarIqbal MD.³

¹Department of Medical Imaging, Subei people's hospital, Medical school of Yangzhou university, Jiangsu, china PR 225001

²Department of Otolaryngology, Subei people's hospital, Medical school of Yangzhou university, Jiangsu, china PR 225001

³Department of General Surgery, Subei people's hospital, Medical school of Yangzhou university, Jiangsu, china PR 225001

†Corresponding author: Ye Jing MD. e-mail: yejing69@yahoo.com

Department of Medical Imaging, Subei People's Hospital, No 98 west Nantong road, Yangzhou city, Jiangsu province, China PR 225001; Tel: (+) 86-514-87373625, 13222676528, 18051061289; Fax: (+) 86-516-87373625.

Abstract

Background: Sturge-Weber syndrome is an embryonal developmental anomaly resulting from errors in mesodermal and ectodermal development. It is caused by a somatic activating mutation occurring in the Guanine nucleotide-binding protein G (q) subunit alpha gene and characterized by vascular malformations present in the skin (port wine stain), eye, and meninges (leptomeningeal angioma). Neuroimaging can provide sufficient information that can guide radiological diagnosis of related brain abnormalities or to differentiate it from other similar types of brain abnormalities.

Objective: To give an overview on literature to determine the role of neuroimaging in diagnosis of Sturge-Weber syndrome and related brain abnormalities.

Methods and materials: A review of the scientific literature was performed in the Medline database (PubMed) from 1988 up to November 2015, using different associations of the following keywords: Sturge weber syndrome, computed tomography, magnetic resonance imaging. Thirty one articles were eventually selected for final review. Two authors reviewed the abstracts of the retrieved records and selected only those related to the aims of the present analysis.

Results and Conclusion: Magnetic resonance imaging with contrast is probably the best imaging test for this condition. However, computed tomography is more sensitive than magnetic resonance imaging in the detection of subcortical calcifications. In addition, functional and nuclear imaging can play significant role to make a more comprehensive diagnosis.

Keywords: Sturge-Weber syndrome; Neurocutaneous disorder; Port wine stain; Computed tomography; Magnetic resonance imaging.

I. Introduction

Sturge-Weber syndrome (SWS) is an embryonal developmental anomaly resulting from errors in mesodermal and ectodermal development. Unlike other neurocutaneous disorders, Sturge-Weber occurs sporadically. It is caused by a somatic activating mutation occurring in the Guanine nucleotide-binding protein G (q) subunit alpha (GNAQ) gene and characterized by vascular malformations present in the skin (port wine stain), eye, and meninges (leptomeningeal angioma).¹ The intracranial vascular anomaly is most often unilateral and involves the occipital and parietal lobes, although it might affect other lobes and spare the most posterior region in some cases.² The birthmark can vary in color from light pink to deep purple and is caused by an overabundance of capillaries around the ophthalmic branch of the trigeminal nerve, just under the surface of the face. Seizures are the most common neurologic complications, varying from 72% to 93% in unilateral and bilateral involvement, respectively.³ Motor development delay, another potential manifestation that worsens the clinical scenario, may be an early neurologic presentation of SWS. Although SWS may eventually progress, many patients remain neurologically normal for months or even years before developing neurological symptoms.⁴ Neuroimaging techniques have been routinely employed in the assessment of children with SWS, and several authors have shown relationships between neuroimaging findings and clinical presentation. A past study with computed tomography (CT) and magnetic resonance imaging (MRI) reported that white matter changes, extent of lobar involvement, and the degree of parenchymal atrophy all correlated with the clinical

status, including seizure control, hemiparesis and the degree of psychomotor development.⁵ Though no current diagnostic tool can reliably predict the clinical course, in this article we have discussed and summarized the conclusive significance of CT and MRI in the detection of brain abnormalities related to SWS.

II. Methodology

A review of the scientific literature was performed in the Medline database (PubMed) from 1988 to November 2015, using different associations of the following keywords: Sturge weber syndrome, CT, MRI. Searching limitations were title/abstract and English language. Editorials, letters and congress abstracts were excluded due to non-sufficient data. Thirty one articles were eventually selected for final review. Two authors reviewed the abstracts of the retrieved records and selected only those related to the aims of the present analysis. All authors carefully analyzed the corresponding full-length articles, and additional referenced papers of interest were identified by hand search and retrieved. This study was approved by the ethical committee of Yangzhou University Health System Institutional Review Board.

III. Discussion

Examinations for SWS include plain skull radiography, CT scanning, MRI, angiography, and nuclear medicine studies.^{6,7,8,9} CT scanning is more sensitive than plain skull radiography and MRI in the detection of subcortical calcifications. However, MRI with contrast is probably the best imaging test. It is superior to CT in the demonstration of abnormal myelination, and it is more sensitive in the demonstration of leptomeningeal enhancement, particularly in the presence of dense cortical calcification on CT scans. In addition, orbital associated malformations are well depicted on contrast-enhanced orbital MRI.^{10,11,12}

CT scans show the tramline gyriform calcification of opposing gyri that underlies the contrast-enhancing leptomeningeal vascular malformation. Cortical enhancement may be difficult to appreciate on CT when cortical calcification is dense. The subjacent white matter may be hypoattenuating on CT scans (Fig.1A and B). The ipsilateral choroid plexus may be enlarged. Enlarged transcortical (medullary) veins are frequently associated with an enlarged choroid glomus.¹³ Other features on CT scans include ipsilateral cortical atrophy, enlargement of the ipsilateral ventricle, and loss of volume of the ipsilateral cranial cavity.¹⁴ Occasionally, the hemicranium is enlarged on the ipsilateral side, with associated enlargement of the cerebrospinal fluid (CSF) space.¹⁵ In short, CT scanning is more sensitive than skull radiography and MRI in the detection subcortical calcifications, and detection is sometimes possible in patients younger than 2 years. Other causes of gyriform intracranial calcification could lead to a false-positive diagnosis.

MRI is the generally accepted preference for diagnosing and monitoring brain involvement, particularly in patients over one year of age. The ideal standard is a T1 and T2-weighted brain MRI with gadolinium contrast and post-contrast fluid attenuated inversion recovery (FLAIR).¹⁶ Neuroimaging can be done proactively, before symptoms even occur. However, in newborns and young infants, these imaging techniques can often lead to false negative results.¹⁷ In T1-weighted image signal of affected region is usually hypointense to isointense, with anatomic volume loss evident at older age while in T2-weighted image signal varies from isointense to mildly hyperintense likely corresponding to ischemic changes in the white matter. Calcifications are better seen in T2-weighted image sequences.

Meanwhile, several new MRI techniques have been developed to allow the assessment of brain abnormalities from different aspects. Susceptibility weighted imaging (SWI) is one of relatively new MRI techniques, specifically designed to be sensitive to small changes in local magnetic susceptibility in the brain tissue (Fig.1C). SWI utilizes the susceptibility difference between tissues to enhance the “native” contrast of different tissue types. Many pathological conditions can be visualized by SWI more clearly than other techniques, including neurovasculature abnormalities, hemorrhage, calcification, iron deposit, and change of oxygenation level induced by blood flow or various disease processes.^{18,19,20,21,22} However, to what extent SWI could complement conventional MRI in the clinical diagnosis and management of SWS is remained unclear. In addition, quantitative brain MR spectroscopy (MRS) and diffusion tensor imaging (DTI) have been used in the characterization of SWS. Differences have been recorded between the abnormal cerebral cortex and the normal contralateral normal cerebral cortex. A choline increase and N -acetylaspartate decrease are observed in a pathologic cortex, while an unaffected cerebral cortex shows no change in the DTI parameters. These changes in the pathologic cortical gray matter in SWS patients probably reflect neuronal loss or dysfunction and demyelination as a result of recurrent seizures.^{23, 24}

Physiologic alterations in SWS can be assessed by using MR perfusion imaging (PWI) and proton spectroscopic imaging (MRSI). PWI changes in SWS indicate cerebral hypoperfusion predominantly due to impaired venous drainage, with only the most severely affected regions showing arterial perfusion deficiency. The severity of cerebral hypoperfusion correlates well with neuronal loss/dysfunction, which is reflected in the severity of neurologic symptoms and disability. The highest correlation is found with the degree of hemiparesis. These parameters may be useful in quantifying disease severity.²⁵ Blood-oxygen-level-dependent (BOLD) MR venography was shown to identify leptomeningeal internal veins in a 4-month-old with SWS when other MR

sequences failed to show any abnormality. Follow-up MRI after the first seizure at the age of 12 months demonstrated strong leptomeningeal enhancement, while BOLD venography revealed abnormal medullary and sub-ependymal veins, as well as deep venous structures. At the time of the second MR scan, signs of cerebral atrophy and calcifications were apparent on CT. The report shows that BOLD venography may allow early diagnosis of venous anomalies in SWS.²²

Abnormal cerebrovenous drainage is associated with ischemia, hypoxia, and glucose deprivation, which can account for progressive neurologic deterioration in SWS. Single-photon emission CT (SPECT) scanning, technetium-99m (^{99m}Tc) hexamethylpropyleneamineoxime (HMPAO) scanning, and fluorodeoxyglucose (FDG) positron emission tomography (PET) scans show diminished perfusion and reduced glucose metabolism in the affected cerebral hemisphere. Approximately 50% of patients with SWS are found to have bihemispheric disease when they are examined with functional imaging, with abnormal perfusion and glucose metabolism being revealed. Widespread abnormalities of cerebral perfusion and glucose metabolism might explain the high prevalence of developmental delay associated with SWS. Hypoperfusion of the involved cerebral hemisphere usually appears in patients older than 1 year.²⁶

SPECT scanning depicts cerebral blood flow asymmetry in infants with SWS, which tends to shift with age. The cortex involved in the vascular malformation is hyperperfused during the first year of life, before the first seizures occur. The characteristic hypoperfusion appears after 1 year of age, even in patients without epilepsy.^{27,1199m} Tc HMPAO imaging is a useful addition to the examination when delineation of the full extent of the abnormality is of particular relevance (eg, before surgery).^{99m} Tc imaging is more likely to depict areas of hypoperfusion, which represent ischemic regions; these areas may act as epileptogenic foci and may not be detected with CT scanning or MRI.

Although SWS is usually categorized with venous malformations, it is an extensive capillary and venous malformation that affects one or sometimes both cerebral hemispheres. Cerebral angiograms show early capillary blush in the areas involved with the pial vascular malformation associated with abnormally large veins in the sub-ependymal and periventricular regions. Enlarged deep medullary veins that drain deep to the sub-ependymal veins are present (Fig.2).The superficial cortical veins in the region of the dystrophic calcification have markedly slow flow as a result of venous thrombosis, but most of the cortical veins are largely absent on the affected side. Rarely, high-flow shunting of arteriovenous malformations is seen. Venous drainage occurs via bizarre, enlarged deep medullary veins into the deep venous system or via a few patent, enlarged cortical veins into the dural venous sinus. The deep veins and dural venous sinus are often not visualized in these patients. Whether the absent veins are congenitally aplastic or occluded as a result of thrombosis is not certain.

Some authorities advocate antiplatelet therapy in SWS, believing that clinical exacerbations may be the result of progressive venous thrombosis, although this has never been clearly documented with conventional angiography. However, progressive dural venous occlusion has been documented with magnetic resonance venography in an infant with SWS, although no luminal thrombus was evident on spin-echo images. So far, observations in SWS do little to clarify the issue of congenital versus acquired abnormality of the intracranial venous system. Other vascular abnormalities seen with SWS include arterial occlusion (rare), segmental venous ectasia, and absent or luminal irregularities and deformities of the deep veins.

Cerebral lobectomy may be considered in some patients. In cases with severe drug-refractory focal epilepsy caused by SWS, promising results have been achieved with hemispherectomy.²⁸ Devlin and associates described the clinical course and outcomes in 33 children who underwent hemispherectomy and concluded that the optimal timing of surgery with respect to age at presentation and the influence of the underlying pathology are only slowly emerging. At surgery, their patients were aged 0.33-17 years.²⁹ Vining and associates from Johns-Hopkins hospital reported their experience with 58 children after hemispherectomy. They concluded that early surgery relieves the burden of constant seizures and allows the child to return to a more-normal life. Kossoff et al concluded that the patient's age at surgery does not have an adverse effect on either seizure or cognitive outcomes.³⁰

Early presymptomatic diagnosis of SWS brain involvement, however, is difficult because standard MRI and CT imaging have low sensitivity in the newborn period and early infancy. A negative head CT and/or contrast enhanced MRI of the brain in a normally developing asymptomatic young infant with a facial (Port wine birthmark (PWB) does not exclude SWS brain involvement. The optimal timing of the first neuroimaging is unknown but current clinical experience suggests that if the child is developing normally, has a normal neurologic exam, no history of seizures, and a normal MRI with contrast after the age of 1 year, that child probably does not have SWS brain involvement. Post-contrast FLAIR and susceptibility-weighted MR imaging may provide additional sensitivity for involved brain areas.^{31,22} Calcification may not be detectable in individuals younger than 2 years. Other causes of gyriform intracranial calcification cannot always be differentiated from those found in SWS. MRI is expensive, it is less widely available, and patients may experience claustrophobia. MRI is contraindicated in patients with certain types of cardiac pacemakers and ferromagnetic prostheses. Klippel-Trenaunay-Weber syndrome and Wyburn-Mason syndrome may cause similar angiographic

appearances. Some previous studies mention that the Diffusion weighted imaging (DWI) and automated formed apparent diffusion coefficient (ADC) have shown some restrictions in affected white matter. Cerebral perfusion defects and areas of hypometabolism are seen with positron emission tomography (PET) in a variety of epileptogenic foci. In light of an appropriate history, the angiographic appearances of SWS can be fairly characteristic, although the role of angiography in the management of SWS is decreasing. However, in patients with medically unresponsive seizures, resection of brain deep to the angioma is sometimes undertaken. In these patients, the identification of large diploic vessels by using angiography can help avoid a difficult craniotomy.

IV. Conclusion

CT and MRI are most often used to identify intracranial abnormalities. Although MRI is not as good as CT scanning in the depiction of calcification, it is superior to CT in the demonstration of abnormal myelination. MRI is much more sensitive in the demonstration of leptomeningeal enhancement, particularly when dense cortical calcification exists on CT scans. Choroidal lesions are well depicted on high-resolution, contrast-enhanced orbital MRIs. MR spectroscopy and diffusion tensor imaging have been used in the characterization of this disease. Functional imaging, nuclear imaging and angiography have additional role to provide a more comprehensive diagnosis or differentiating the similar types of brain abnormalities.

Key points:

1. CT scanning is more sensitive than plain skull radiography and MRI in the detection of subcortical calcifications and detection is sometimes possible in patients younger than 2 years.
2. Magnetic resonance imaging with contrast is probably the best imaging test for diagnosis of SWS related cerebral vascular malformations.
3. ^{99m}Tc imaging is more likely to depict areas of hypoperfusion, which represent ischemic regions; these areas may act as epileptogenic foci and may not be detected with CT scanning or MRI.

Abbreviations

SWS: Sturge weber syndrome
GNAQ: Guanine nucleotide-binding protein G (q) subunit alpha
CT: Computed tomography
MRI: Magnetic resonance imaging
FLAIR: Fluid attenuated inversion recovery
SWI: Susceptibility weighted imaging
MRS: Magnetic resonance spectroscopy
DTI: Diffusion tensor imaging
PWI: Perfusion weighted imaging
MRSI: Magnetic resonance proton spectroscopic imaging
BOLD: Blood-oxygen-level-dependent
SPECT: Single-photon emission CT
^{99m}Tc: Technetium-99m
HMPAO: Hexamethylpropyleneamineoxime
FDG: Fluorodeoxyglucose
PET: Positron emission tomography
PWB: Port wine birthmark
DWI: Diffusion weighted imaging
ADC: Apparent diffusion coefficient

Acknowledgements

This study received no funding.

References

- [1]. Bebin EM, Gomez MR. Prognosis in Sturge-Weber disease: comparison of unihemispheric and bihemispheric involvement. *J Child Neurol.*1988; 3:181–184.
- [2]. Thomas-Sohl KA, Vaslow DF, Maria BL. Sturge-Weber syndrome: a review. *Pediatr Neurol.*2004; 30:303–310.
- [3]. Roach ES. Neurocutaneous syndromes. *Pediatr Clin North Am.*1992; 39:591–620.
- [4]. DilberC, Tasdemir HA, Dagdemir A. et al. Sturge-Weber syndrome involved frontoparietal region without facial nevus. *Pediatr Neurol.*2002; 26:387–390.
- [5]. Marti-Bonmati L, Menor F, Mulas F. The Sturge-Weber syndrome: correlation between the clinical status and radiological CT and MRI findings. *Childs Nerv Syst.*1993; 9:107–109.
- [6]. Tong KA, Ashwal S, Obenaus A. et al. Susceptibility-Weighted MR Imaging: A Review of Clinical Applications in Children. *Am J Neuroradiol.*2008;29: 9-17.

- [7]. Jordan LC, Wityk RJ, Dowling MM. et al. Transcranial Doppler ultrasound in children with Sturge-weber syndrome. *J Child Neurol.* 2008 23:137-143.
- [8]. Juhász C, Lai C, Behen ME. et al. Chugani DC. White matter volume as a major predictor of cognitive function in Sturge-Weber syndrome. *Arch Neurol.* 2007 64:1169-1174.
- [9]. Hatfield LA, Crone NE, Kossoff EH. et al. Quantitative EEG asymmetry correlates with clinical severity in unilateral Sturge-Weber syndrome. *Epilepsia.* 2007;48:191-195.
- [10]. Whitehead MT, Vezina G. Osseous intramedullary signal alteration and enhancement in Sturge-Weber syndrome: an early diagnostic clue. *Neuroradiology.*2015; 57:395-400.
- [11]. Kamson DO, Juhász C, Shin J. et al. Patterns of structural reorganization of the corticospinal tract in children with Sturge-Weber syndrome. *Pediatr Neurol.* 2014;50:337-342.
- [12]. Cagneaux M, Paoli V, Blanchard G. et al. Pre- and postnatal imaging of early cerebral damage in Sturge-Weber syndrome. *PediatrRadiol.* 2013;43:1536-1539.
- [13]. Yamazaki K, Hirata K. [Dyke-Davidoff-Masson syndrome]. *RyoikibetsuShokogunShirizu.* 2000;30:177-178.
- [14]. Tasdemir HA, Incesu L, Yazicioglu AK. Dyke-Davidoff-Masson syndrome. *Clin Imaging.* 2002; 26:13-17.
- [15]. Kochar DK, Jain N, Sharma BV. Dyke-Davidoff Masson syndrome: neuroimage. *Neurol India.* 2001;49:417.
- [16]. Nabbout R, Juhász C. Sturge-Weber syndrome. *Hand Clin Neurol.* 2013; 111:315–321.
- [17]. Ewen JB, Kossoff EH, Crone NE, et al. Use of quantitative EEG in infants with port-wine birthmark to assess for Sturge-Weber brain involvement. *Clin Neurophysiol.*2009; 120:1433–1440.
- [18]. Haacke EM, Xu Y, Cheng YC, Reichenbach JR. Susceptibility weighted imaging (SWI) *Magn Res Med.*2004; 52:612–618.
- [19]. Reichenbach JR, Venkatesan R, Schillinger DJ. et al. Small vessels in the human brain: MR venography with deoxyhemoglobin as an intrinsic contrast agent. *Radiology.*1997; 204:272–279.
- [20]. Wang Y, Yu Y, Li D, et al. Artery and vein separation using susceptibility-dependent phase in contrast-enhanced MRA. *J MagnReson Imaging.*2000; 12:661–670.
- [21]. Sehgal V, Delproposito Z, Haacke EM. Et al. Clinical applications of neuroimaging with susceptibility-weighted imaging. *J MagnReson Imaging.*2005; 22:439–450.
- [22]. Mentzel HJ, Dieckmann A, Fitzek C. et al. Early diagnosis of cerebral involvement in Sturge-Weber syndrome using high-resolution BOLD MR venography. *Pediatr Radiol.*2005; 35:85–90.
- [23]. Sijens PE, Gieteling EW, Meiners LC. et al. Diffusion tensor imaging and magnetic resonance spectroscopy of the brain in a patient with Sturge-Weber syndrome. *Acta Radiol.*2006; 47:972-976.
- [24]. Batista CE, Chugani HT, Hu J. et al. Magnetic resonance spectroscopic imaging detects abnormalities in normal-appearing frontal lobe of patients with Sturge-Weber syndrome. *J Neuroimaging.*2008; 18:306-313.
- [25]. Lin DD, Barker PB, Hatfield LA, Comi AM. Dynamic MR perfusion and proton MR spectroscopic imaging in Sturge-Weber syndrome: correlation with neurological symptoms. *J MagnReson Imaging.*2006; 24:274-281.
- [26]. Chugani HT. The role of PET in childhood epilepsy. *J Child Neurol.* 1994; 9:82-88.
- [27]. Pinton F, Chiron C, Enjolras O. Early single photon emission computed tomography in Sturge-Weber syndrome. *J NeurolNeurosurg Psychiatry.*1997;63:616-621.
- [28]. Tuxhorn IE, Pannek HW. Epilepsy surgery in bilateral Sturge-Weber syndrome. *Pediatr Neurol.*2002; 26:394-397.
- [29]. Devlin AM, Cross JH, Harkness W. Clinical outcomes of hemispherectomy for epilepsy in childhood and adolescence. *Brain.*2003; 126:556-566.
- [30]. Kossoff EH, Buck C, Freeman JM. Outcomes of 32 hemispherectomies for Sturge-Weber syndrome worldwide. *Neurology.*2002; 59:1735-1738.
- [31]. Griffiths PD, Coley SC, Romanowski CA, et al. Contrast-enhanced fluid-attenuated inversion recovery imaging for leptomeningeal disease in children. *Am J Neuroradiol.*2003; 24:719–723.

Figures

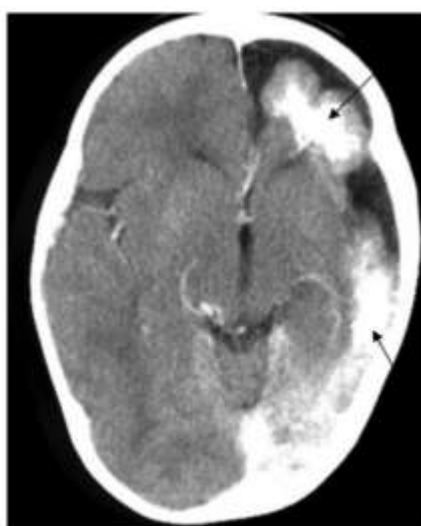


Figure 1A: Non-enhanced axial Head CT demonstrating significant left sided atrophy and cortical, sub-cortical calcification in a patient with Sturge-Weber syndrome (arrows).

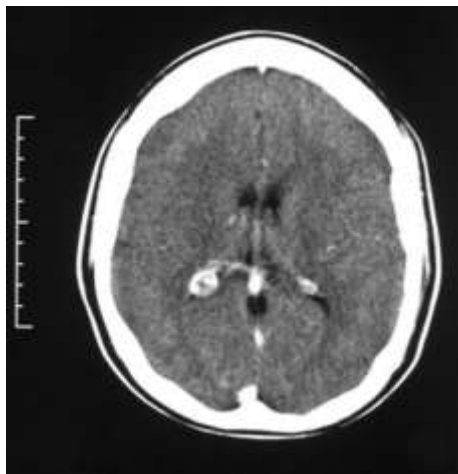


Figure1B: Axial contrast-enhanced CT scan through the occipital horns of the lateral ventricles shows right cerebral atrophy and an enlarged right choroid plexus in a patient with Sturge-Weber syndrome.

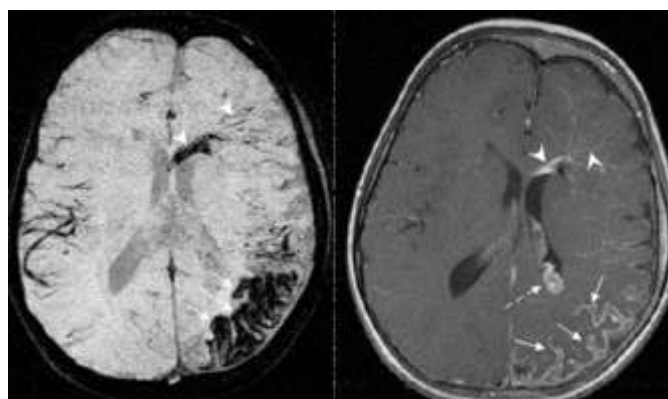


Figure1C: Image sequence: SWI (left) and T1-Gd (right). The abnormal gyri manifest as hypointensity on SWI image and extensive leptomeningeal enhancement on T1-Gd images (solid arrow). Abnormalities on SWI are seen more within the cortex, while abnormalities on T1-Gd are seen more overlying the cortex, and slight hypointensities are seen along cortex. Both SWI and T1-Gd images reveal the winding transmedullary veins and abnormal periventricular vein (arrow head), and brain atrophy. However, the enlarged choroid plexus is visualized only by T1-Gd images (dashed arrow).

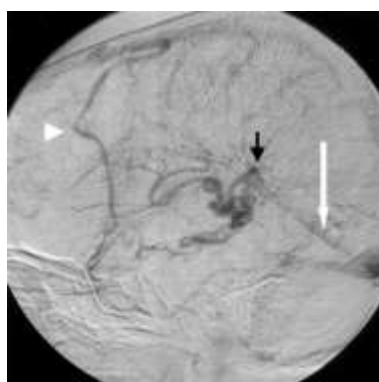


Fig.2: Cerebral angiogram (left carotid injection). There is a relative absence of superficial cortical veins but numerous radially orientated transmedullary veins draining into enlarged thalamostriate and mesencephalic veins and thence into an ectatic internal cerebral vein. The distal internal cerebral vein pursues an abnormal corkscrew course, and drains into Galenic (black arrow) and straight sinus (white arrow). The abnormal draining veins have a caput medusa appearance characteristic of a developmental venous anomaly. A prominent cortical vein of Trolard is noted (white arrowhead).